

This is a repository copy of *Fermionic correlations as metric distances : a useful tool for materials science*.

White Rose Research Online URL for this paper:  
<http://eprints.whiterose.ac.uk/120069/>

Version: Accepted Version

---

**Article:**

D'Amico, Irene [orcid.org/0000-0002-4794-1348](https://orcid.org/0000-0002-4794-1348), Pittalis, Stefano and Marocchi, Simone (2017) Fermionic correlations as metric distances : a useful tool for materials science. PHYSICAL REVIEW MATERIALS. 043801. pp. 1-5. ISSN 2475-9953

<https://doi.org/10.1103/PhysRevMaterials.1.043801>

---

**Reuse**

Items deposited in White Rose Research Online are protected by copyright, with all rights reserved unless indicated otherwise. They may be downloaded and/or printed for private study, or other acts as permitted by national copyright laws. The publisher or other rights holders may allow further reproduction and re-use of the full text version. This is indicated by the licence information on the White Rose Research Online record for the item.

**Takedown**

If you consider content in White Rose Research Online to be in breach of UK law, please notify us by emailing [eprints@whiterose.ac.uk](mailto:eprints@whiterose.ac.uk) including the URL of the record and the reason for the withdrawal request.

# Fermionic correlations as metric distances: a useful tool for materials science

Simone Marocchi,<sup>1</sup> Stefano Pittalis,<sup>2</sup> and Irene D’Amico<sup>1,3</sup>

<sup>1</sup>*Instituto de Física de São Carlos, Universidade de São Paulo, CP 369, 13560-970, São Carlos, SP, Brasil.\**

<sup>2</sup>*CNR-Istituto di Nanoscienze, Via Campi 213A, I-41125 Modena, Italy<sup>†</sup>*

<sup>3</sup>*Department of Physics and York Centre for Quantum Technologies,  
University of York, York YO10 5DD, United Kingdom<sup>‡</sup>*

(Dated: August 7, 2017)

We introduce a rigorous, physically appealing, and practical way to measure distances between exchange-only correlations of interacting many-electron systems, which works regardless of their size and inhomogeneity. We show that this distance captures fundamental physical features such as the periodicity of atomic elements, and that it can be used to effectively and efficiently analyze the performance of density functional approximations. We suggest that this metric can find useful applications in high-throughput materials design.

PACS numbers: 31.15.E-, 31.15.V-, 71.15.Mb, 03.65.-w

Discovering innovative materials and engineering devices with targeted properties involve substantial experimental and theoretical efforts. Their progress ultimately relies on our understanding of the physics at the nanoscale. Atomistically, the possible constituents and their combinations are vast. One can often focus on the state of electrons within the Born-Oppenheimer approximation, however a too direct computational approach is in general unpractical, because of the presence of many degrees of freedom and the fact that these are interrelated in a non-trivial fashion. Density Functional Theory (DFT) proposes an alternative by transforming the problem of determining interacting many-body system properties into the solution of the Kohn-Sham (KS) equations, which only involve auxiliary non-interacting particles [1–3]. Practically, the KS approach relies on the possibility of devising approximate forms for the exchange-correlation (xc) energy – a functional of the particle density. This functional embodies the effects of many-body correlations due to the intrinsic anti-symmetry of the many-electron state and to the electrostatic electron-electron repulsions; it also accounts for the auxiliary KS system being non-interacting. Within this context, we wish to expose the usefulness of introducing metric spaces to analyze many-body correlations – when the protocol to define these spaces is both rigorous and based on quantities with a deep physical meaning.

There is an increasing interest in the use of metrics to explore quantum mechanical systems [4–10], and appropriate (‘natural’) metrics for particle densities, wavefunctions, and external potentials [4, 7] already shed light on (previously unknown) features of the mappings at the base of the Hohenberg-Kohn theorem, the cornerstone of DFT. Among the ultimate goals of DFT applications is the determination of properties such as total energies, ionization potentials, electron affinities, the fundamental gaps, and lattice distances of crystalline structures. All these quantities can be computed accurately only if the

relevant two-body correlations are properly captured by the underlying approximations. The xc-energy, at the core of the KS DFT approach, can be expressed in terms the aforementioned two-body correlations by means of the xc-hole function as defined in the so-called adiabatic coupling-constant integration [1–3]. Furthermore, the xc-hole can be split into a correlation and an exchange (x) component. Here, we focus on an exchange-only analysis of this quantity (more details follow below), which is useful for dealing with relatively weakly correlated systems’ ground-states. First, we will introduce a ‘natural’ distance for the x-hole and show that it captures fundamental physical features such as the periodicity of atomic elements; afterwards we will also demonstrate that it can be used to analyze effectively and efficiently the performance of density functional approximations.

Let us briefly remind a few fundamental definitions [11]. The exchange-hole (x-hole) has an expression

$$n_x(\mathbf{r}, \mathbf{r}') = - \frac{\sum_{\sigma} |\gamma_{\sigma}(\mathbf{r}, \mathbf{r}')|^2}{n(\mathbf{r})} \quad (1)$$

which can be evaluated once the KS one-body reduced-density-matrix (1BRDM)

$$\gamma_{\sigma}(\mathbf{r}, \mathbf{r}') = \sum_k f_{k\sigma} \psi_{k\sigma}(\mathbf{r}) \psi_{k\sigma}^*(\mathbf{r}') \quad (2)$$

is known. This, in turn, only requires the knowledge of the *occupied* single-particle orbitals  $\psi_{k,\sigma}(\mathbf{r})$ . Here,  $f_{k\sigma}$  are occupation numbers and  $\sigma$  is the  $z$ -projection of the spin index [12]. At the denominator of Eq. (1), the particle density is determined from the trace  $n(\mathbf{r}) = \sum_{\sigma} \gamma_{\sigma}(\mathbf{r}, \mathbf{r})$ . Note that the calculation of the x-energy,  $E_x$ , can be based on the knowledge of the system-averaged x-hole,  $\langle n_x \rangle$ , as follows

$$E_x = 2\pi \int_0^{\infty} u du \langle n_x \rangle(u) \quad (3)$$

where

$$\langle n_x \rangle(u) := \int d\mathbf{r} n(\mathbf{r}) n_x(\mathbf{r}, u), \quad (4)$$

with

$$n_x(\mathbf{r}, u) := \frac{1}{4\pi} \int d\Omega_{\mathbf{u}} n_x(\mathbf{r}, \mathbf{r} + \mathbf{u}) \quad (5)$$

being the spherical-average of the x-hole, and  $\Omega_{\mathbf{u}}$  the solid angle defined by  $\mathbf{u}$  around  $\mathbf{r}$ . Therefore, practical calculations in DFT can be enabled by providing approximations for  $\langle n_x \rangle(u)$ . Sensible approximations must satisfy important exact conditions. In this respect, it is well known that the property

$$\int_0^\infty 4\pi u^2 du \langle n_x \rangle(u) = -N \quad (6)$$

together with the point-wise negativity condition are of outmost importance. These two properties can be combined, giving raise to the constraint

$$\int_0^\infty 4\pi u^2 du |\langle n_x \rangle(u)| = N. \quad (7)$$

*Crucially*, through Eq. (7) and by following the protocol for deriving ‘natural’ metrics of Ref. 5, *these same conditions allow us to define the ‘natural’ distance* between two given system-averaged x-hole functions

$$D_x[\langle n_x^{(1)} \rangle, \langle n_x^{(2)} \rangle] := 4\pi \int_0^\infty u^2 du |\langle n_x^{(1)} \rangle(u) - \langle n_x^{(2)} \rangle(u)|. \quad (8)$$

Eq. (8) is the key result of the present work. We emphasize that the same exact conditions that are essential to explain surprisingly good performance of even very rough DFT approximations, allow us to introduce a rigorous metric: we expect then this metric to capture the essential physics of exchange-only correlations.

Eq. (8) summarizes the difference between the exchange-only correlations of two many-body systems into a *single number*. While differences of exchange energies could be thought too as ‘single numbers’ to estimate the difference between the exchange in two systems, Eq. (8) not only rigorously satisfy the mathematical properties of a distance [13] but also enables a comparative analysis of the systems far more detailed than the claim that they have the same exchange energy – the examples illustrated below will provide a vivid illustration of this point. By the metrics’ axioms,  $D_x = 0$  if and only if the two systems considered have the *same* system-averaged x-hole (modulo irrelevant differences over sets of vanishing measure). For non vanishing distances, Eq. (8) implies a *well defined maximum*, given by the sum of the two systems’ particle numbers. This can be evinced from Eq. (8) and Eq. (7) by considering two systems of particle numbers  $N_1$  and  $N_2$  and for which the system-averaged x-holes do not overlap: in this case  $D_x = N_1 + N_2$ . Because

the system-averaged x-holes have definite sign, this also corresponds to the maximum distance between the two systems. This property implies that the x-hole distance between two systems gives us an *non-arbitrary* ‘absolute’ measure of their closeness, as their distance can be recast in terms of a *percentage of their maximum possible distance*.

Furthermore, Eq. (8) implies a very effective geometrical structure of the physical Fock space. Consider to apply Eq. (8) to compute the distance between the *exact* system-averaged x-holes of two different systems. This distance represents a measure of the difference of the exchange-only correlations between two systems. A system with no particles may be thought as a point, say, at the center of the Fock space. Because of Eq. (7), all the other systems will be distributed at a fixed distance equals to the number of particles in the systems. Thus, the overall Fock space can be thought as the union of disjoint ‘onion-like’ shells: systems with same number of particles are on the same shell; systems whose external potential differ only by a constant are separated by a vanishing distance (i.e., they occupy the same point) as the orbitals and therefore the 1BDM and corresponding particle densities do not change. Exchange-holes and therefore their distances are unchanged if each single-particle orbital is multiplied by the same constant phase. This embodies the fact that both the Schrödinger equation and the DFT framework are invariant under global gauge transformations [14]. Systems will be on different shells if they have different particle numbers: the distances acquire minimum value (i.e., the absolute value of the difference of the shell radii) if the systems ‘face each other’; and they acquire maximum value (i.e., the sum of the shell radii), if the systems are ‘on opposite poles’ [15]. Of course, the configurations which generate maximum, and – for systems on different shells – minimum distances are not unique.

Finally, let us consider the evaluation of Eq. (8) using some approximate  $\langle n_x \rangle$ . Since Eq. (7) must be fulfilled, proper approximations preserve the mentioned onion-like structure of the Fock space. Also the minimum and maximum distances are unchanged, but the configurations at which these occur may vary from the exact case. The errors due to the approximation may be viewed as fictitious displacements of the systems from their exact locations on the aforementioned shells. Having the possibility to quantify these errors through a rigorously defined distance that can also be visualized is *per se* very appealing. In the rest of this Letter, we will give explicit examples of how powerful this approach can be.

We start by considering a set of systems for which the exact x-holes can be calculated: we will discuss the exact results as well as compare and contrast these with corresponding results from DFT approximations. Here we shall consider popular approximations for  $\langle n_x \rangle$ : the Local-Density Approximation (LDA), the General-

ized Gradient Approximation (GGA), and the Meta-GGA (MGGA). The LDA takes as a reference the xc energy densities of the homogeneous electron gas; GGA and MGGA are non-empirical refinements which aim at capturing the effects of system inhomogeneities – those neglected within the LDA – while progressively satisfying a larger set of exact conditions. LDA forms make use only of the particle density  $n(\mathbf{r})$  as input; GGAs also use the reduced dimensionless gradient,  $s(\mathbf{r}) = |\nabla n(\mathbf{r})|/\{2[3\pi^2]^{1/3}n(\mathbf{r})^{4/3}\}$ ;  $n(\mathbf{r})$  and  $s(\mathbf{r})$ , the kinetic-energy density  $\tau = \sum_{k\sigma} f_{k\sigma} |\nabla\psi_{k\sigma}(\mathbf{r})|^2$  and, possibly, the laplacian of the particle density may be exploited in MG-GAs. MGGA forms are then considered to be the most accurate approximations among these three. As representative approximations for  $\langle n_x \rangle$ , we choose the Ernzerhof and Perdew version of PW92 (LDA) [16], PBE (GGA) [16], and TPSS (MGGA) [17, 18] forms.

Fig. 1 shows the distances of the exact  $\langle n_x \rangle$  (solid line) from a reference system chosen (arbitrarily) at  $Z^{ref} = 50$  for the isoelectronic Helium-like sequence [19]. Distances from the reference system increase monotonically for both increasing and decreasing values of  $Z$ . As the distance increases the spatial overlap of the related system-averaged x-holes decreases. The system-averaged x-holes  $\langle n_x(u) \rangle$  describes the system-averaged electron depletion observed at separation  $u$  from a reference electron due to the effect of electron-electron exchange, so an increasing distance  $D_x$  implies systems with an increasingly different spatial exchange pattern. When there is no overlap between these patterns, their distance saturates at its maximum, which is  $D_x^{max} = 4$  for the set of systems of Fig. 1. Next we check how the trend for the exact exchange of Helium-like ions is reproduced by the approximations (dotted, dashed and dashed-dotted lines, as labelled in Fig. 1). While the qualitative general trend is mostly reproduced, we note that, quantitatively, the fewer exact conditions an approximation satisfies, the higher the inaccuracy [20], which in fact increases as we move from MGGA to GGA to LDA. In particular LDA becomes unable to reproduce, even qualitatively, the saturation to maximum distance, despite considering ion’s nuclear charges as large as  $Z = 2000$ .

Distances can be used also to perform ‘point-by-point’ exact-to-approximated comparisons, by directly computing the distance between exact and approximated exchange for each system. Fig. 2 shows the distances of approximated  $\langle n_x \rangle$  from the corresponding exact quantity for each ion in the isoelectronic Helium-like sequence. As the electrons get strongly confined around the nucleus, the effect of the electron-electron interaction becomes negligible with respect to an external potential which increases linearly with  $Z$ . In this way, the non-interacting limit of an infinitely charged ion is approached. Interestingly errors with respect to the exact results quickly saturate at a finite constant. For LDA and GGA, these

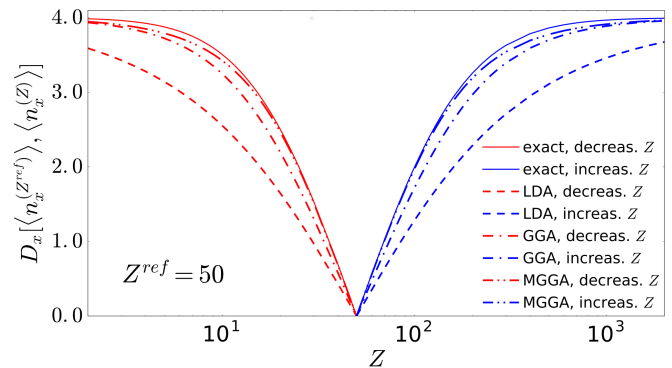


Figure 1. The x-hole distance  $D_x$  from the reference state  $Z^{ref} = 50$  is plotted against the atomic number  $Z$  for the Helium-like ion series. The exact results correspond to the solid lines, LDA to the dashed, GGA to the dashed-dot, and MGGA to the dashed-dot-dot lines.

errors may be mainly related to spurious self interactions. Notably, although the considered MGGA gives rather accurate x-energies for two-electron systems, it is obvious that a sizable error still persists at the level of  $\langle n_x \rangle$ . Importantly, the use of ‘natural’ metrics allows us to *quantify* what we mean by ‘sizable’, by expressing the error as a *percentage of the maximum distance*. In the case at hand then a 10% error threshold would correspond to  $D_x = 0.4$  (dashed black line). We can then assert that for the Helium-like ion series both GGA and MGGA always provide results which are closer than 10% to the exact ones (about 7.8% for GGA and between 4.0% and 3.0% for MGGA), while LDA estimates, at about 24.0% of  $D_x^{max}$ , are always well above the chosen error threshold.

Consistently with the general expectation, both in Fig. 2 and Fig. 1, the GGA performs in between the MGGA and LDA; however our method and results show in an immediate and appealing visual way how substantial is the improvement obtained in going from an LDA to a GGA. The improvement of the MGGA over the GGA is not as large as from LDA to GGA, but still significant.

To the end of DFT practitioners, it is important to clarify under which circumstances numerically ‘cheaper’ approximations could be used in place of more accurate but computationally more involved approaches. Toward this goal, in the rest of this letter, we show how the metric for the x-hole can be used to efficiently compare the performance of different DFT approximations on large sets of systems. In the process we will also show how  $D_x$  can be used to capture and compare physical trends within a large set of systems.

First we focus on physical trends within a set of systems, and so we consider distances between x-holes of *different* systems calculated using the *same* approximation. Fig. 3 shows distances between neutral atoms with atomic numbers  $Z$  and  $Z - 1$ . Moving along the rows of the periodic table, the periodicity is well reflected in

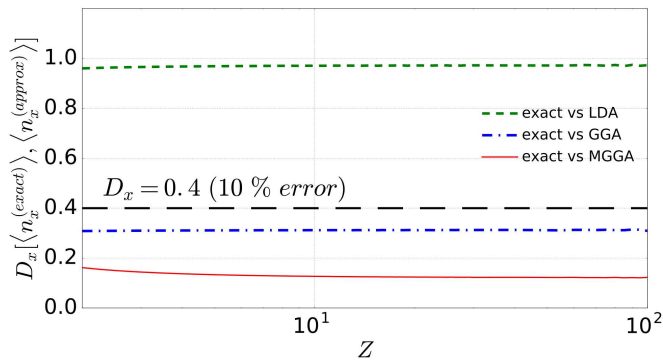


Figure 2. The x-hole distance  $D_x$  is plotted against the atomic number  $Z$  for the Helium-like ion series. For each  $Z$ , the distance is calculated between the exact x-hole and several approximated x-holes (LDA, GGA and MGGA), as labelled. The black, dashed line represents 10% percent of the maximum distance from the exact x-hole.

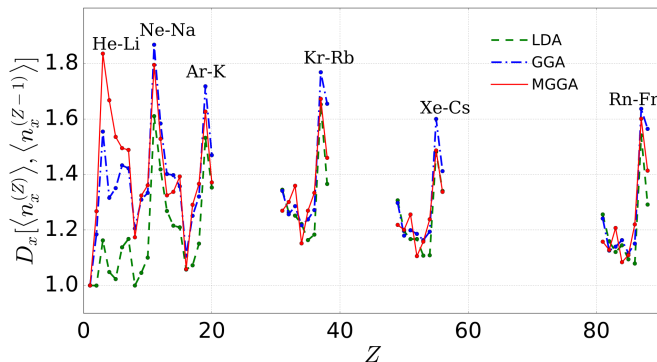


Figure 3. The x-hole distance  $D_x$  between atoms with atomic numbers  $Z$  and  $Z - 1$  is plotted against  $Z$  for the  $s$ - and  $p$ -blocks of the periodic table. The distance are calculated for LDA, GGA and MGGA, as labelled. The distances between the end and beginning of consecutive periods are explicitly labelled with the corresponding atoms. All the input Kohn-Sham quantities have been obtained using the APE code [21]. We allow for spin-polarization by performing Spin-DFT calculations [12]. We used logarithmic spaced grids and cubic spline interpolation [22] to calculate the x-hole distance between different atoms. All the densities and x-hole sum rules were tested within  $10^{-4}$ .

the behaviors of  $D_x$  for MGGA (solid line), the most accurate approximation here considered. For example the curves characteristically peak when considering the distance between the exchange of the last atom of one row and the first of the next (as labelled in Fig. 3). This behavior follows from the sharp change of the corresponding atomic sizes. The curves also display characteristic minima at every start of double occupancy of  $p$ -shells: as the fourth  $p$ -electron is introduced, the atomic radius does not change significantly. This implies that the x-hole distance from the previous atom sharply decreases. Significant deviations are observed for LDA results for atoms in the first two rows. We explain this by not-

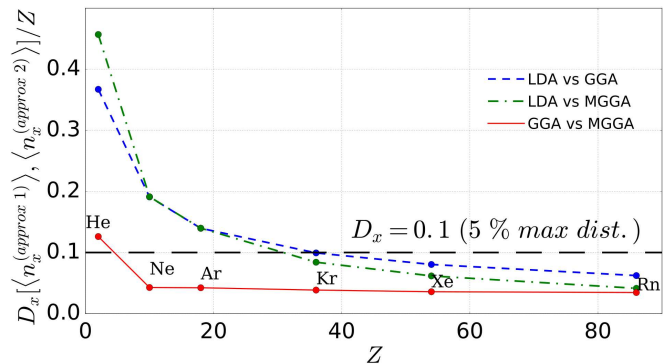


Figure 4. The x-holes distance  $D_x$  is plotted against the atomic number  $Z$  for the noble gas series. The distances are calculated between different approximations to the same x-hole for all atom, as labelled, and are rescaled by the number of electrons. The black, dashed line marks 5% of the maximum possible distance. All the input Kohn-Sham quantities have been obtained using the APE code [21].

ing that self-interaction errors become larger in small systems, and electrons of light elements tend to behave rather differently from the electrons in a homogenous gas. GGA improves over this by accounting better for density inhomogeneity, but it is still quite poor for the smaller  $Z$ -values. For larger values of  $Z$ , the trends of LDA and GGA looks qualitatively more similar to MGGA results, though, as  $Z$  increases, maximum and minimum features related to the filling of the  $p$ -shells gets displaced with respect to MGGA positions.

Next, we wish to show how distances can lead to direct comparison between different approximations: here distances are calculated between *different* approximations applied to the *same* system, e.g. the same atom. In Fig. 4, we report these distances for the noble gases. First thing to notice is that the distances among the various approximations decrease substantially with increasing  $Z$ . This is related to the fact that, in all the considered approximations, the leading contribution to the semiclassical expansion of the exchange energies is provided through LDA [23]. The remaining differences can be attributed to high-orders contributions, more related to system inhomogeneities. Consistently, thus, the GGA and MGGA result to be closer to each other than to the LDA. We can now define an error threshold to establish the parameter region for which LDA and GGA would be a good-enough ‘cheaper’ substitute for MGGA. As our best results are already approximated, we consider in this case a threshold of 5% of the maximum possible distance, which corresponds in this case to  $D_x/Z < 0.1$  (black dashed line in Fig. 4). It is immediate to see then that while LDA would be appropriate only for the heaviest three, GGA would be a good choice for all noble gasses except Helium.

In summary, we have presented a new way for rigorously and quantitatively compare exchange-only correla-

tions of different systems. We have given evidence that by the use of a ‘natural’ metrics it is possible to effectively and efficiently characterize exchange-only correlations in many-electron systems. Our metric based on the exchange hole could have important practical applications in evaluating DFT approximations. For example, our results suggest that among the available approximations for the system-averaged exchange-hole, the meta-GGA performs best, and could be used in evaluating distances for systems widely different in size and level of inhomogeneity. Our x-hole metric could also help guiding high-throughput materials design [24], e.g. for searching in large configurational spaces or for validating the reproducibility of a collaborative database of electronic calculations, independently from the different methodology, quantum package or hardware used [25]. ‘Natural’ metrics such as this or the one for the particle density [4] might also be used to ensure that newly developed functionals optimize, together with the total energies, other key physical quantities, helping reverting the trend recently described in [26].

We thank Prof. Luiz Nunes de Oliveira for fruitful discussions. I.D. acknowledge support by the Royal Society through the Newton Advanced Fellowship scheme (Grant no. NA140436). I.D. and S.M. were supported by the Conselho Nacional de Desenvolvimento Científico e Tecnológico (CNPq, Grant: PVEProcesso: 401414/2014-0) and S.P. was supported by the European Community through the FP7s Marie-Curie Incoming-International Fellowship, Grant agreement No. 623413.

---

\* simonemarocchi@ifsc.usp.br

† stefano.pittalis@nano.cnr.it

‡ irene.damico@york.ac.uk

- [1] W. Kohn, *Rev. Mod. Phys.* **71**, 1253 (1999).
- [2] K. Capelle, *Braz. J. Phys.* **36**, 1318 (2006), ISSN 0103-9733.
- [3] W. Koch and M. C. Holthausen, *A Chemists Guide to Density Functional Theory* (Wiley-VCH Verlag GmbH, 2001).
- [4] I. D’Amico, J. P. Coe, V. V. França, and K. Capelle, *Phys. Rev. Lett.* **106**, 050401 (2011).
- [5] P. M. Sharp and I. D’Amico, *Phys. Rev. B* **89**, 115137 (2014).
- [6] P. M. Sharp and I. D’Amico, *Phys. Rev. A* **92**, 032509 (2015).
- [7] P. M. Sharp and I. D’Amico, *Phys. Rev. A* **94**, 062509 (2016).
- [8] D. P. Pires, M. Cianciaruso, L. C. Céleri, G. Adesso, and D. O. Soares-Pinto, *Phys. Rev. X* **6**, 021031 (2016).
- [9] C. J. Turner, K. Meichanetzidis, Z. Papic, and J. K. Pachos, *Nat. Commun.*, doi=10.1038/ncomms14926 (2017).
- [10] K. Funo, J.-N. Zhang, C. Chatou, K. Kim, M. Ueda, and A. del Campo, *Phys. Rev. Lett.* **118**, 100602 (2017).
- [11] For the sake of simplicity, we restrict ourselves to the cases for which the Kohn-Sham state is a single Slater determinant.
- [12] In the standard formulation of Kohn-Sham DFT, the occupation numbers,  $f_{k\sigma}$ , take integer values (0 or 1). Fractional values are also admitted in the sense of its ensemble generalization. In this work, we restrict to closed-shell systems or to situations with globally collinear spin polarizations. In the latter case, one must take into consideration that the x-hole acquires a dependence on the spin polarization. The spin-dependent x-hole can be expressed in terms of the spin-unpolarized x-hole by means of the spin-scaling relation [18, 27] as follows
- $$n_x[n_\uparrow, n_\downarrow](\mathbf{r}, \mathbf{r}') = \sum_{\sigma} \frac{n_{\sigma}(\mathbf{r})}{n(\mathbf{r})} n_x[2n_{\sigma}](\mathbf{r}, \mathbf{r}').$$
- [13] W. A. Sutherland, *Time-Dependent Density Functional Theory* (Oxford University Press, 2009).
- [14] For discussing invariance under more general gauge transformations, one should admit additional couplings to proper external gauge fields and adopt the corresponding extensions of the DFT frameworks; as done, for example, in Current-DFT and Spin-CDFT. [28–30].
- [15] The onion-shell geometry characterizes *all* ‘natural’ metrics, as a consequence of the protocol defined to derive them. A detailed discussion, including a discussion of the polar angle characterizing the distance between two systems, can be found in Ref. 5.
- [16] M. Ernzerhof and J. P. Perdew, *J. Chem. Phys.* **109**, 3313 (1998).
- [17] J. P. Perdew, J. Tao, V. N. Staroverov, and G. E. Scuseria, *J. Chem. Phys.* **120**, 6898 (2004).
- [18] L. A. Constantin, J. P. Perdew, and J. Tao, *Phys. Rev. B* **73**, 205104 (2006).
- [19] The isoelectronic Helium-like sequence was solved exactly combining the approaches taken by Accad et al. [31] and Coe et al. [32].
- [20] A. J. Garza, G. E. Scuseria, A. Ruzsinszky, J. Sun, and J. P. Perdew, *Mol. Phys.* **114**, 928 (2016).
- [21] M. J. T. Oliveira and F. Nogueira, *Comp. Phys. Commun.* **178**, 524 (2008), ISSN 0010-4655.
- [22] P. Dierckx, *Curve and Surface Fitting with Splines* (Oxford University Press, Inc., New York, NY, USA, 1993), ISBN 0-19-853441-8.
- [23] P. Elliott and K. Burke, *Can. J. Chem.* **87**, 1485 (2009).
- [24] S. Curtarolo, G. L. W. Hart, M. B. Nardelli, N. Mingo, S. Sanvito, and O. Levy, *Nat. Mater.* **12**, 191 (2013).
- [25] C. E. Calderon, J. J. Plata, C. Toher, C. Oses, O. Levy, M. Fornari, A. Natan, M. J. Mehl, G. Hart, M. B. Nardelli, et al., *Comp. Mater. Science* **108, Part A**, 233 (2015), ISSN 0927-0256.
- [26] M. G. Medvedev, I. S. Bushmarinov, J. Sun, J. P. Perdew, and K. A. Lyssenko, *Science* **355**, 49 (2017).
- [27] J. P. Perdew, K. Burke, and Y. Wang, *Phys. Rev. B* **54**, 16533 (1996).
- [28] G. Vignale and M. Rasolt, *Phys. Rev. Lett.* **59**, 2360 (1987).
- [29] G. Vignale and M. Rasolt, *Phys. Rev. B* **37**, 10685 (1988).
- [30] K. Bencheikh, *J. Phys. A: Math. Gen.* **36**, 11929 (2003).
- [31] Y. Accad, C. L. Pekeris, and B. Schiff, *Phys. Rev. A* **4**, 516 (1971).
- [32] J. P. Coe, K. Capelle, and I. D’Amico, *Phys. Rev. A* **79**, 032504 (2009).